Evaluation of neutron total and capture cross sections on ^{99}Tc in the unresolved resonance region

Nobuyuki Iwamoto[1,a] and Tatsuya Katabuchi[2]

[1] Nuclear Data Center, Nuclear Science and Engineering Center, Japan Atomic Energy Agency, 2-4 Shirakata, Tokai, Ibaraki 319-1195, Japan
[2] Laboratory for Advanced Nuclear Energy, Tokyo Institute of Technology, Meguro-ku, Tokyo 152-8550, Japan

Abstract. Long-lived fission product Technetium-99 is one of the most important radioisotopes for nuclear transmutation. The reliable nuclear data are indispensable for a wide energy range up to a few MeV, in order to develop environmental load reducing technology. The statistical analyses of resolved resonances were performed by using the truncated Porter-Thomas distribution, coupled-channels optical model, nuclear level density model and Bayes' theorem on conditional probability. The total and capture cross sections were calculated by a nuclear reaction model code CCONE. The resulting cross sections have statistical consistency between the resolved and unresolved resonance regions. The evaluated capture data reproduce those recently measured at ANNRI of J-PARC/MLF above resolved resonance region up to 800 keV.

1. Introduction

Radioactive Technetium-99 has a characteristic of long half-life (2.11×10^5 yr). This long-lived fission product is generated by e.g. ^{235}U fission in nuclear power plants and the cumulative fission yield exceeds 6% [1]. Hence, it is considered that ^{99}Tc is one of the most important fission products and that it should be reduced by a transmutation system of nuclear waste via e.g., neutron capture reaction.

The experiments by time-of-flight and lead slowing-down time techniques have been performed for capture cross section up to the unresolved resonance region [2–6]. Their measured data show a dispersion of ∼20% in that region. Above 70 keV the cross section measurement was only done by Macklin [4]. However, the experiment by the time-of-flight method was recently made with a NaI(Tl) spectrometer of ANNRI installed at the Materials and Life Science Experimental Facility (MLF) of J-PARC [7]. The capture cross section was obtained over a wide region from the thermal energy up to several hundred keV energies.

Gunsing et al. [8] made neutron transmission measurement by the time-of-flight method and extracted the resolved resonance parameters for 659 resonances up to 10 keV [8]. Clear assignment of a resonance orbital angular momentum to s- or p-wave is hard from experimental data except for a special case that resonance interference is observed. They adopted the Bayesian analysis on conditional probability [9,10]. A key to the analysis is a large difference in penetrabilities between s- and p-wave resonances.

A nuclear data project entitled as "Research and development for Accuracy Improvement of neutron nuclear data on Minor ACtinides (AIMAC)" is being performed in Japan. The present work aims at high quality evaluation based on close collaboration with experimenters. A method adopted by Noguere et al. [11] was revised and applied to the statistical analysis of resolved resonances, in order to obtain resonance properties and to finally derive total and capture cross sections.

2. Methodology of analyses

The small number of p-wave resonances assigned by Gunsing et al. may indicate that most of the p-wave resonances is still missing. This suggests that their averaged values cannot be derived only from the resonance information. Hence, different approaches from those of Gunsing et al. were adopted in this work. The present work adopted the following procedure of (i)–(iv) to obtain the statistical values of s- and p-wave resonances. Initial resonance parameters of resonance energy E, neutron width $g\Gamma_n$ and orbital angular momentum l were adopted from Gunsing et al. [8].

(i) The truncated Porter-Thomas distribution was used to obtain an averaged s-wave neutron strength function S_0 and level spacing D_0. The distribution provides the number $N(X_{t0})$ of s-wave resonances which have the reduced neutron width $g\Gamma_n^0$ larger than the threshold value X_{t0} and is expressed by

$$N(X_{t0}) = \left(\frac{E_{\max} - E_{\min}}{D_0} + 1\right)\left[1 - \mathrm{erf}\left(\sqrt{\frac{X_{t0}}{2S_0 D_0}}\right)\right], \quad (1)$$

where $E_{\max}$ and $E_{\min}$ are the maximum and minimum energies for the relevant energy range of resonance region, erf is the usual error function.

(ii) The p-wave neutron strength function was determined by using an optical model of the CCONE code [12]. The optical potential form was taken from

[a] e-mail: iwamoto.nobuyuki@jaea.go.jp

Kunieda et al. [13]. The coupled-channels approach was employed. The ground state (spin-parity $9/2^+$) was coupled with excited levels 727 keV ($11/2^+$) and 762 keV ($13/2^+$) with deformation parameters $\beta_2 = 0.153$ and $\beta_4 = 0.056$. The experimental data of Foster and Glasgow [14] in the MeV region and the value of S_0 obtained in (i) were reproduced with modified parameters of the optical model potential. An averaged p-wave strength function S_1 was obtained at an incident neutron energy of 1 keV.

(iii) The composite level density formula of Gilbert and Cameron [15] was used with the reproduction of the D_0 value. The p-wave level spacing D_1 was derived at the neutron separation energy of ^{100}Tc.

(iv) The fixed values of S_0, D_0, S_1 and D_1 were applied to assigning the orbital angular momentum. The Bayes' theorem on conditional probabilities was used for this purpose. The probability that a resonance with neutron width $g\Gamma_n$ is a p-wave is expressed by

$$P(l=1|g\Gamma_n) = \left(1 + \frac{P(l=0)P(g\Gamma_n|l=0)}{P(l=1)P(g\Gamma_n|l=1)}\right)^{-1}, \quad (2)$$

if it is considered that d-wave resonances do not have an influence in the considered energy range. The determined D_0 and D_1 were taken into account, in order to give the a priori probabilities $P(l=0)$ and $P(l=1)$ that the resonance is an s- or a p-wave one. The neutron strength function of l-wave resonance is described with an average reduced neutron width $\langle g\Gamma_n^l \rangle$ by

$$S_l = \frac{\langle g\Gamma_n^l \rangle}{(2l+1)D_l}. \quad (3)$$

The ratio between probabilities of neutron width for s- and p-wave resonances, $P(g\Gamma_n|l=0)$ and $P(g\Gamma_n|l=1)$, is written as

$$\frac{P(g\Gamma_n|l=0)}{P(g\Gamma_n|l=1)} = \frac{\sqrt{\frac{2v_1 S_1 D_1}{S_0 D_0}}\exp\left[-\frac{g\Gamma_n}{2\sqrt{E}}\left(\frac{1}{S_0 D_0} - \frac{1}{2v_1 S_1 D_1}\right)\right]}{\frac{1}{2}\left(1+\sqrt{\frac{\pi g\Gamma_n}{4v_1 S_1 D_1 \sqrt{E}}}\right)}, \quad (4)$$

where v_1 is related to the penetration factor of a p-wave. The factor is defined by

$$v_1 = \frac{(kR')^2}{1+(kR')^2}, \quad (5)$$

where k is the neutron wave number, R' is the scattering radius, which was adopted to be 7.17 fm determined by Gunsing et al. in this work. If the probability ratio of Eq. (4) is unity, and defining the ratio of the probabilities $P(l=0)/P(l=1)$ as the ratio of the corresponding level densities, the limit of the probability $P(l=1|g\Gamma_n)$ is finally expressed as

$$P(l=1|g\Gamma_n) = \frac{D_0}{D_0 + D_1}. \quad (6)$$

If the probability of a resonance was larger than this limit, the resonance was assigned to a p-wave. This procedure of (i)-(iv) was iterated until the assignment of orbital angular momentum was fixed. The resulting numbers of s- and p-wave resonances and statistical values are summarized in Table 1, in which comparisons are made with those of Mughabghab [16] and RIPL-3 [17] as well as Gunsing et al.

Table 1. Results of statistical analysis for resonances.

	Gunsing et al.	Mughabghab	RIPL-3	Present
s-wave	518	—	—	473
p-wave	141	—	—	186
$10^4 S_0$	0.52 ± 0.08	0.49 ± 0.06	0.50 ± 0.06	0.53
D_0 (eV)	12.0 ± 1.3	12.8 ± 0.5	14.0 ± 1.2	11.0
$10^4 S_1$	3.8 ± 0.8	5.8 ± 0.8	5.3 ± 0.5	5.3
D_1 (eV)	6.0	6.8 ± 0.3		5.7

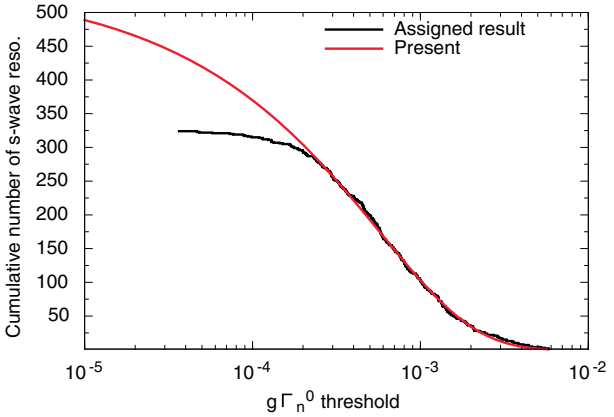

Figure 1. Truncated Porter-Thomas distribution for s-wave resonances (up to 6 keV) as a function of a threshold value of reduced neutron width.

The neutron transmission coefficient after convergence was applied to a statistical model in CCONE. Neutron capture cross section and gamma-ray spectrum were finally obtained by evaluating calculated results with experimental data.

3. Results

Figure 1 shows the result of fitting to the cumulative number of s-wave resonances with a reduced neutron width which is larger than a threshold value by using the truncated Porter-Thomas distribution of Eq. (1). The result finally assigned to an s-wave resonance is plotted as histogram. The statistical values of the s-wave resonances were obtained as $S_0 = 0.53 \times 10^{-4}$ and $D_0 = 11.0$ eV. These values are almost consistent with the original data of Gunsing et al. and those of compilations [16, 17] as shown in Table 1.

The total cross section has been measured only by Foster and Glasgow [14] above the resolved resonance region (i.e., 6 keV in JENDL-4.0). Figure 2 shows comparison of the present result with the data of Foster and Glasgow, together with those of JENDL-4.0, ENDF/B-VII.1 and JEFF-3.2. The cross sections of the evaluated libraries in the resonance region below 7 keV are averaged over the energy bin width. In that region, the difference in the averaged cross sections mainly comes from that in the scattering radius adopted in the libraries (i.e., 6.7 fm in JENDL-4.0, 7.15 fm in ENDF/B-VII.1 and 7.3 fm in JEFF-3.2). The present cross section, together with the best

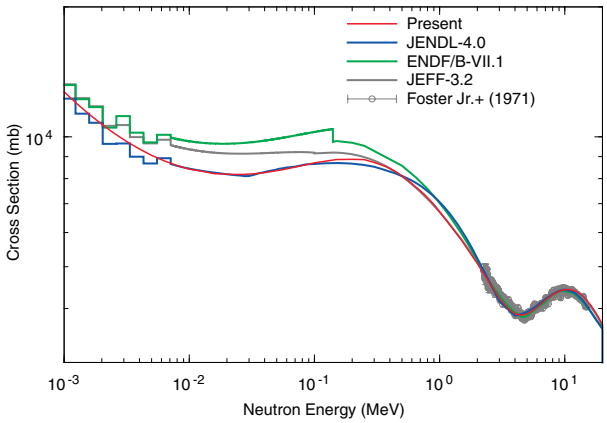

Figure 2. Comparison of the present total cross section with experimental data, together with those of evaluated data.

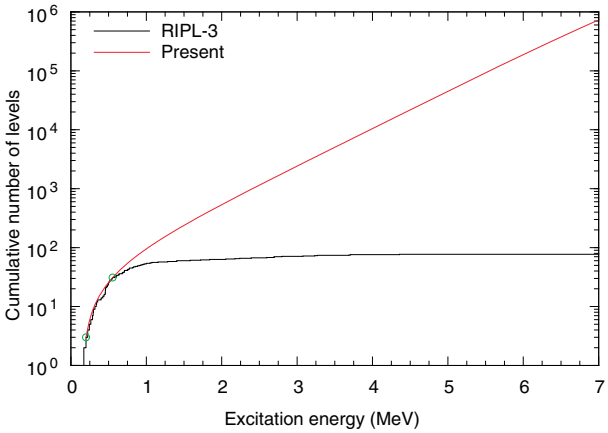

Figure 3. Fitted result (solid line) to the cumulative number of nuclear levels for ^{100}Tc by the level density model based on a Gilbert-Cameron formula. The known levels are represented as histogram. The circles indicates the levels adopted for the fitting. The neutron binding energy of ^{100}Tc is 6.764 MeV.

estimated S_0 value, is in good agreement with the data of Foster and Glasgow.

Figure 3 shows the calculated result of a level density model based on the Gilbert-Cameron formula which was fitted to cumulative number of nuclear levels for ^{100}Tc. The open circles represent the upper and lower energy boundaries for the fitting. The level density in the fitting region can be described by the constant temperature model. The energy-dependent level density parameter with shell correction was adopted in the Fermi-gas model which was taken from Mengoni and Nakajima [18]. The value of D_0 was reproduced by modifying the level density parameter.

Figure 2 shows the distribution of neutron width divided by the square root of neutron energy. The s- and p-wave resonances are represented by circle and square symbols, respectively. The present results and those of Gunsing et al. are illustrated by filled and open symbols, respectively. The average values of neutron width for s-, p- and d-wave resonances are expressed by

$$\frac{\langle g\Gamma_n \rangle}{\sqrt{E}} = (2l+1)v_l S_l D_l. \quad (7)$$

Difference from the assignment of Gunsing et al. is found in the border region between the s- and p-wave resonances. The resulting numbers of s- and p-wave resonances are

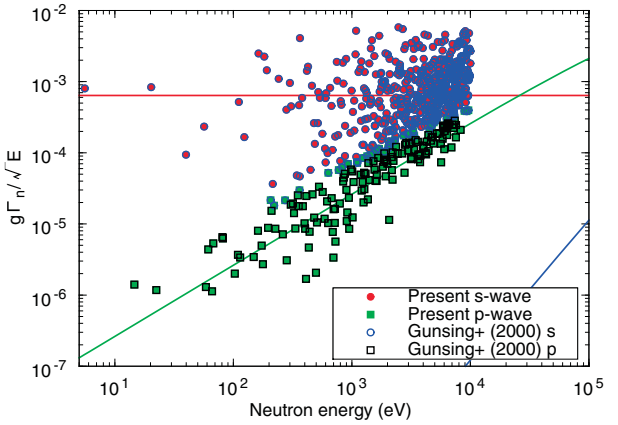

Figure 4. Distribution of neutron width divided by the square root of neutron energy. Filled and open symbols represent the results of this work and Gunsing et al., respectively. Circles and squares stands for the s- and p-wave resonances, respectively. The lines show the average values for s, p- and d-wave resonances, respectively.

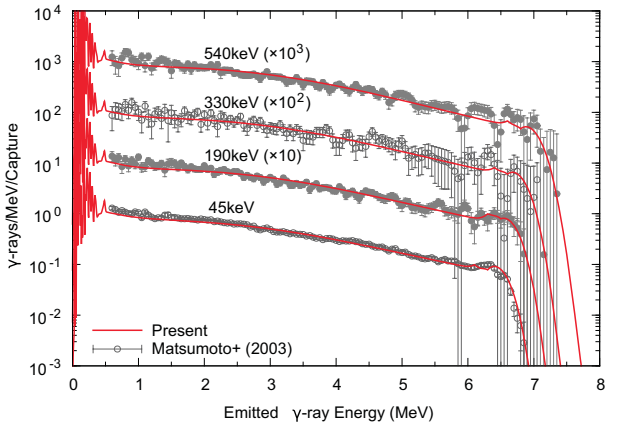

Figure 5. Comparison of the present capture gamma-ray spectra with experimental data in the neutron energy range of 45–540 keV.

473 and 186, respectively, as listed in Table 1. The present number of p-wave resonance is increased by 45. This change may be ascribed to the different fitting methodology used to obtain S_0 and D_0. The average value of a d-wave resonance is smaller by more than three orders of magnitude, in comparison with that of a p-wave one.

Figure 5 shows comparison of the present capture gamma-ray spectra with the data of Matsumoto et al. [2] at average neutron energies of 45, 190, 330 and 540 keV. A modified Lorentzian form was adopted for gamma strength function. The parameters of gamma-ray strength function for M1 radiation was modified to reproduce the measured data. The present result obtains a good agreement with the measured slope.

Figure 6 presents the final result of capture cross section. The present data are consistent with those of the recent measurement at ANNRI/J-PARC [7]. However, the other experimental data are systematically smaller than the present results by 40% at a maximum. The origin of the difference should be investigated to minimize the dispersion among the measured data.

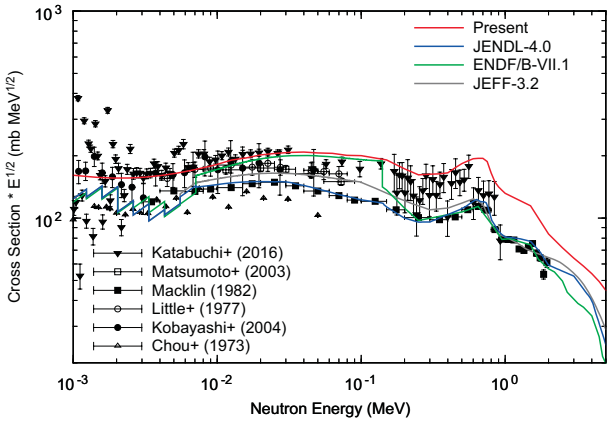

Figure 6. Comparison of the present capture cross section with experimental data, together with those of evaluated data.

4. Summary

The present work analyzed the statistical properties of resonances for radioactive ^{99}Tc by combining the truncated Porter-Thomas distribution, coupled-channels optical model, nuclear level density model of Gilbert-Cameron formalism and Bayes' theorem on conditional probability. The procedure was iterated to derive the neutron strength functions and level spacings for an s- and a p-wave resonance until convergence was achieved for the orbital angular momentum. The resulting numbers of s- and p-wave resonances were 473 and 186. The latter was increased by 30% in comparison with the number of p-wave resonances derived by Gunsing et al. The total and capture cross sections were determined by the nuclear reaction model code CCONE, and were obtained with consistency of statistical values between the resolved and unresolved resonance regions. The present capture cross section is in agreement with the data measured at ANNRI of J-PARC/MLF in the unresolved resonance region up to 800 keV.

The authors are grateful for the financial support of "Research and development for accuracy improvement of neutron nuclear data on minor actinides (AIMAC)" project entrusted to Japan Atomic Energy Agency by Ministry of Education, Culture, Sports, Science and Technology of Japan (MEXT).

References

[1] J. Katakura, JAEA-Data/Code 2011-025 (2012)
[2] T. Matsumoto, M. Igashira, T. Ohsaki, J. Nucl. Sci. Technol. **40**[2], 61–68 (2003)
[3] K. Kobayashi, S. Lee, S. Yamamoto, T. Kawano, Nucl. Sci. Eng. **146**, 209–220 (2004)
[4] R. L. Macklin, Nucl. Sci. Eng. **81**, 520–524 (1982)
[5] J.-C. Chou, H. Werle, J. Nucl. Energy **27**, 811–823 (1973)
[6] R.C. Little, R.C. Block, Transactions of the American Nuclear Society **26**, 574 (1977)
[7] T. Katabuchi et al., this proceedings
[8] F. Gunsing, A. Lepretre, C. Mounier, C. Raepsaet, Phys. Rev. **C61**, 054608 (2000)
[9] L.M. Bollinger, G.E. Thomas, Phys. Rev. **171**, 1293–1297 (1968)
[10] M. Gyulassy, R.J. Howerton, S.T. Perkins, Report No. UCRL-50400, Vol. 11 (1972)
[11] G. Noguere, Phys. Rev. **C81**, 044607 (2010)
[12] O. Iwamoto, N. Iwamoto, S. Kunieda, F. Minato, K. Shibata, Nucl. Data Sheets **131**, 259 (2016)
[13] S. Kunieda et al., J. Nucl. Sci. Technol. **44**, 838–852 (2007)
[14] D.G. Foster, Jr, D.W. Glasgow, Phys. Rev. **C3**, 576–603 (1971)
[15] A. Gilbert, A.G.W. Cameron, Can. J. Phys. **43**, 1446 (1965)
[16] S.F. Mughabghab, Atlas of Neutron Resonances - Resonance Parameters and Thermal Cross Sections $Z = 1 - 100$. Elsevier (2006)
[17] R. Capote et al., Nucl. Data Sheets **110**, 3107 (2009)
[18] A. Mengoni, Y. Nakajima, J. Nucl. Sci. Technol. **31**, 151 (1994)